1995

Estimation of underwater scalar PAR : models and measurements in lakes

Yin Zhong
Lehigh University

AUTHOR:

Zhong, Yin

TITLE:

Estimation of Underwater Scalar Par: Models and Measurements in Lakes

DATE: May 28, 1995

Estimation of Underwater Scalar PAR:

Models and Measurements in Lakes

by

Yin Zhong

A Thesis

Presented to the Graduate Committee

of Lehigh University

in Candidacy for the Degree of

Master of Science

in

Environmental Sciences

Lehigh University

May 1995

This thesis is accepted in partial fulfillment of the requirements for the Master of Science.

Date 5/9/95

Professor Bruce R. Hargreaves
Thesis Advisor

Doctor Robert E. Moeller
Committee Member

Professor Donald P. Morris
Committee Member

Professor Bobb Carson
Chairman of Department

ACKNOWLEDGEMENTS

I wish to thank Dr. Bruce R. Hargreaves, my thesis advisor, for his close guidance and understanding of me, as an international student from a different culture, during my graduate studies at Lehigh University. I also wish to thank Dr. Robert E. Moeller and Dr. Donald P. Morris for their valuable advise on my thesis writing and presentations and great help in field measurements. This research was supported by an Andrew W. Mellon Foundation grant to Dr. Craig E. Williamson which supported the Pocono Comparative Lakes Program. Special thanks are given to Dr. Bobb Carson and Dr. Paul B. Myers for their support and encouragement in my life and studies at Lehigh University. I can never forget our office staff Laurie Cambiotti and Nancy Roman who are always ready to help with a smile. Last, I would like to give a spiritual hug to my family for their love, encouragement, and support.

TABLE OF CONTENTS

Abstract	p. 1
1. Introduction	p. 2
2. Methodology	p. 7
2.1 Basic Approach	p. 7
2.2 Model Development	p. 7
2.3 Instruments	p. 10
2.4 Data Collection	p. 10
3. Results	p. 11
3.1 Measurements of Q_o/Q_d	p. 11
3.2 Test of model A	p. 12
3.3 Test of model B1 and B2	p. 14
4. Discussion	p. 15
5. Conclusions	p. 16
6. Tables	p. 17-23
7. Figures	p. 24-40
8. References	p. 41-42
9. Significant symbols	p. 43
10. Vita	p. 44

LIST OF FIGURES

Fig. 1 Underwater light availability.

Fig. 2 Optical processes in atmosphere-lake system.

Fig. 3 Variation of the Q_0/Q_d ratio in Giles (3a) and Lacawac (3b).

Fig. 4 Comparison of the cosine and scalar sensors.

Fig. 5 Responses of the cosine and scalar sensors.

Fig. 6 Environmental influences on the Q_0/Q_d ratio.

Fig. 7 Model A: a Monte Carlo computer simulation of underwater light field.

Fig. 8 Submersible irradiance sensor (Li-Cor Inc., Lincoln, Nebraska, USA) in a lowering frame.

Fig. 9 The measurements of the Q_0/Q_d ratio in Giles (9a) and Lacawac (9b).

Fig. 10 Irradiance reflectance in Giles (10a) and Lacawac (10b).

Fig. 11 The effect of reflectance on the ratio in Giles (11a) and Lacawac (11b).

Fig. 12 The effect of sun-angle on the ratio in Giles (12a) and Lacawac (12b).

Fig. 13 The predictions of the ratio with model A, B1, and B2 in Giles (13a-e).

Fig. 14 The predictions of the ratio with model A, B1, and B2 in Lacawac (14a-e).

Fig. 15 Estimation of the Q_0 irradiance in Giles (15a) and Lacawac (15b).

LIST OF TABLES

Table 1 Data availability.

Table 2 Comparison of the scalar sensor and cosine sensor

Table 3 The measurements of the Q_0/Q_d ratio: averages and standard deviations.

Table 4 The average of the irradiance reflectance in the lakes.

Table 5 Errors of Q_0/Q_d predictions caused by using averaged R.

Table 6 Errors of Q_0/Q_d predictions caused by sun-angle.

Table 7 The predictions of the ratio by model A: averages and standard deviations.

Table 8 Errors of model A.

Table 9 The predictions of the ratio by model B1 and B2: Averaged with depths.

Table 10 Errors of model B1.

Table 11 Errors of model B2.

Table 12 Comparison of the model errors

Table 13 Statistical test of the models.

Table 14 Applications and limitations of the models.

ABSTRACT

The ratio of underwater scalar irradiance to underwater downwelling irradiance (Q_0/Q_d) has been measured in two Pocono mountain lakes and computed with two kinds of spreadsheet models developed from published theoretical and empirical equations. The measurements show the ratio varies from 1.1 to 2.2, and averaged about 1.5 in contrast to some published statement that the ratio is less than 1.2 or essentially 1. One model (model A) uses irradiance reflectance, sun-angle, and refractive index of water to predict the ratio at 3 particular depths with interpolation to solve for intermediate depths. Another model (model B), assumes that the ratio is constant through a water column at a given time, requires the accurate measurement or estimation at one depth, and gives the predicted ratios at all depths. The predictions of model A deviate from the measurements by ±5-14% over the dates tested; and those of model B deviates by ±3-11%. A statistical test shows that 50% of all the predictions differ significantly from lake measurements. The significant errors of the predictions are partly caused by the rapid fluctuations in the light fields not fully recorded by the instrument, especially at upper layers of the waters. Model A can be used without a scalar light sensor involved in the measurements. The smaller error of model B is achieved by using a pair of scalar sensor and cosine sensor measurements at a single depth below the surface. In contrast to published models, the models proposed in this thesis are enable convenient practical use in estimation of underwater light fields .

1. INTRODUCTION

Water quality has been a major issue in water resource protection and management in all the countries of the world. The algae (photosynthetic) production in waters is one of the most important indicators in evaluation of water quality evaluation, of which eutrophic conditions represent one extreme and oligotrophic conditions the other.

Underwater light availability is one of the major factors limiting photosynthetic production because the only energy source of photosynthesis is sunlight which is attenuating with depth in water (Fig.1). People have become more interested in understanding the underwater light field, because the light availability is strongly related to the photosynthetic production (Platt & Sathyendranath, 1988) such that production can be predicted by depths and time of day if light field is understood (Smith *et al.*, 1989).

There is a fast pace in the development of optical instrumentation for the purpose of photosynthesis estimation in natural waters. The automatic light-profilers, the PUV500 and PNF300 (Biospherical Instruments, Inc.), for instances, represents an advanced design for measuring underwater light fields by simultaneously obtaining different kinds of spatially continuous measurements of light, temperature, depth, and natural fluorescence in the field. Alternatively, the method of numerical modeling of underwater light field has also been commonly applied in estimation of underwater irradiances and radiances (Plass & Kattawar, 1969, 1972; Kirk, 1981; Gordon, 1987; Stavn & Weidemann, 1988; Mobley, 1989; Mobley, et al., 1993) for cases when an accurate instrumental measurement of underwater light cannot be obtained.

The difficulty of accurate measurements of the light availability is due, partly, to the complexity of underwater light field and partly to the limitation of the light sensors. The underwater light field is complicated by both optical processes above, at, and below the air-water interface and optical properties of natural waters. Generalized interactions between photons and media (air, water-body and its components) are shown in Figure 2. The processes of refraction, reflection, and scattering will change both the angle and intensity of the direct sunlight, while the absorption by algae, yellow substances, other particles, and water itself will only reduced the light intensity. Although the refraction occurs only at the interface, the rest of the processes will occur at any depth, with the result that in an underwater environment the photons may travel in all directions. Algal cells have evolved to adapt to these light conditions by matching the properties of light absorbing pigments in the chloroplast so that all the photons (within the wavelengths from 400~700 nm) are equally useful in photosynthesis regardless of the direction from which they come (Kirk, 1994a).

Irradiance Q (at a point on a plane surface) is the radiant flux incident on an infinitesimal element of a surface, containing the point under consideration, divided by the area of that element (Kirk, 1994a). In practice, the photon flux on a plane surface is divided by the area of the surface. Irradiance has units of W m^{-2}, or quanta (photons) s^{-1} m^{-2}, or mol quanta (or photons) s^{-1} m^{-2}, where 1.0 mol photons is 6.02×10^{23} (Avogadro's number) photons. One mole of photons is frequently referred to as an *Einstein*.

The *scalar irradiance*, Q_0, has long been advocated as the best measure of underwater light availability for estimating photosynthetic production. It is defined as the

integral of the radiance distribution at a point over all directions about the point. In practice, the area in scalar irradiance units is the area of a plane surface always perpendicular to each photon.

The scalar (or 4π) light sensor is not favored by most of the limnologists and oceanographers for profiling natural waters though it is commercially available. The sensor is physically fragile due to designed shape and material used, and is subject to error in its readings due to the shading by a large base of a profiler. It is usually not available with a light profiling instrument. Most light profiling instruments use a cosine (or 2π) light sensor. Table 1 summarizes the reasons for differences in popularity of the scalar and cosine sensors and Figure 4 shows their typical shape. The popularity of the cosine sensor is due, in no small part, to the relative ease in their measurement and the reliability of readings (Jerome, *et al.*, 1989).

A cosine sensor is capable of measuring vector irradiances, downwelling and upwelling irradiances for instance. *Downward irradiance*, Q_d, and *upward irradiance*, Q_u, are the values of the irradiance on the upper and the lower faces, respectively, of a horizontal surface. Q_d is the irradiance due to the downwelling light stream and Q_u is that due to the upwelling light stream. Figure 5 describes the response to angle of light.

In practice, the value of Q_0 is sometimes replaced by measurements of Q_d after assuming the ratio of Q_0/Q_d to be less than 1.2 (Morel, 1991). However, it has been reported that variation of the ratio is between about 1.25 and 10 measured at 13 depths from above surface to the depth of 30 m at different time of day in the Irish Sea in Spring in 1987 (Jordan, 1988). Theoretically, the Q_0/Q_d ratio will be equal to 1 if a

collimated beam light comes at the direction normal to the surface of the cosine sensor only. The ratio will be 4 if the light is completely diffused. The ratio has no upper limit if directional light is coming from an angle not normal to the cosine sensor surface. Therefore, the change of the ratio of directed light intensity to diffused light intensity determines the change of the Q_0/Q_d ratio.

In the field, the 2π sensor response will decrease with the increase of the zenith angle of sun light. This cosine effect will become more complicated due to the influences of environmental factors, such as time, atmosphere, clouds, wind, interface roughness, water transparency, and shading which all affect the ratio of direct sunlight to diffused sunlight (Fig. 6). Although the major component of the solar irradiances is downwelling irradiance, replacing Q_0 with Q_d will underestimate the underwater light availability seriously (Kirk, 1994a), and a constant ratio of Q_0/Q_d should not be used without any research.

Another means to obtain the estimation of the scalar irradiance is modeling underwater light fields. A computer simulation technique, the Monte Carlo method, determines the fates of large numbers of photons by computing the fate of each photon and then computing the average behavior of the total photon flux. This method has been used by both oceanographers and limnologists (Kirk, 1994). C. D. Mobley, *et al* (1993) have compared 7 numerical models of underwater light field which are applied to the solutions of seven problems drawn from optical oceanography, which include: highly absorbing and highly scattering waters, scattering by molecules and by particulate, stratified water, atmospheric effects, surface-wave effects, bottom effects and Raman

scattering. They also show that the errors of model outputs (Q_d, Q_0, and upward radiance) are usually smaller than the experimental errors made in measuring irradiances when using current oceanographic instrumentation.

Several theoretical expressions of the Q_0/Q_d ratio have been proposed (Preisendorfer, 1976; Prieur and Sathyendranath, 1981; Jerome *et al.*, 1988; Morel, 1991; Kirk, 1994;). J. Kirk (1981), who has conducted bio-optical studies in inland, coastal, and oceanic waters since 1970's, developed a Monte Carlo calculation procedure for computer modelling of the penetration of light into turbid, colored waters of the type commonly found on the Australian continent. For monochromatic light, he described the underwater light field in terms of average cosine (μ-bar) and irradiance reflectance (R), as a function of optical depth (Z_e) at a given ratio of scattering to absorption (b/a), and as a function of b/a at a given Z_e. More applicable for practical use, Jerome, *et al.* (1988), used Monte Carlo simulation to calculate the ratio of Q_0/Q_d at depths corresponding to the 100, 10, and 1% downwelling irradiance levels (optical depths of Z_{100}, Z_{10}, and Z_1), and defined the ratio of Q_0/Q_d as a function of irradiance reflectance, solar zenith angle, refractive index, and optical depth. In a later experiment, J. Kirk (1994 a&b) found that for media with b/a ranging from 0.3 to 30, diffuse attenuation coefficient of scalar irradiance (K_0) is very close to that of downwelling irradiance (K_d) with a range of the K_d/K_0 from 0.967 to 1.06. He further pointed out that the measured value of K_d can therefore be taken as a reasonable estimate of the value of K_0, and used to predict the attenuation of scalar irradiance with depth. Gordon (1989) has proposed a method for estimating Q_{0d}/Q_d, the ratio of downwelling scalar irradiance to downwelling irradiance using atmospheric

conditions or simply sun angle. Atmospheric conditions can be measured by cosine recording with a cosine sensor exposed to both sky and sun, and then with sun light shaded.

The purpose of this thesis is to develop computer models for Q_0/Q_d ratio prediction for practical use in lakes in order to obtain the most accurate estimate of the underwater scalar light field when a scalar light sensor is not available or when fluctuationing conditions make scalar measurements impractical.

2. METHODOLOGY

2.1. Basic Approach

We developed three practical models (A, B1, & B2). A fourth option became known to us late in the project; it is described briefly but was not tested. We measured Q_0, Q_d, and other parameters required as input to models A and B. We analyzed and tested the performances of the models. Measurements are made in two lakes, L. Giles (lat. N41^{0}22'34", long. W75^{0}5'33", elev. 428 m) and L. Lacawac (lat. N41^{0}22'57"; long. W75^{0}17'35"; elev. 439 m) in the Pocono Mountains in Pennsylvania. The area, maximum depth, average PAR attenuation coefficient are 0.481 km^2, 24 m, and 0.2 m^{-1} in L. Giles, and 0.214 km^2, 13 m, and 0.7 m^{-1} in L. Lacawac (Moeller, *et al.*, 1995).

2.2. Model Development

Model A.

Jerome *et al.*'s Q_0/Q_d model has been selected as model A for its best applicability. According to Jerome *et al.* (1988), the only factors needed to be measured

and input into the model are the irradiance reflectance, R (= Q_u/Q_d), solar zenith angle (or sun-angle, measured from zenith), θ, optical depth, Z_{∞}, and refractive index of water, N_w.

Theoretically, the lower the irradiance reflectance, the smaller will be the Q_0/Q_d ratio; the smaller the sun-angle, the smaller will be the ratio; and the shallower the depth, the smaller will be the ratio. Figure 7 shows that at a given sun-angle and a given depth, the Q_0/Q_d ratio is a function of reflectance, R, only.

Equations in model A will apply to three depths: Z_{100} (the depth just below the water surface), Z_{10} (the depth where only 10% of surface light is available), and Z_1 (the depth of 1% surface light):

(1) At the surface (Z_{100}):

$$Q_0/Q_d\{R,\theta\} = (1.068/\mu_0 - 0.068)(1 + 3.13R) \qquad (1.1)$$

where $\mu_0 = \cos\theta_0$ is the cosine of the in-water refracted angle θ_0 for the incident radiation distribution characterized by sun-angle θ, and since

$\cos\theta_0 = (1 - \sin^2\theta_0)^{0.5}$ and

$\sin\theta/\sin\theta_0 = N_w$ where N_w is the refraction index N of a material (water, here).

The combined equation for μ_0 is,

$$\mu_0 = (1 - \sin^2\theta/N_w^2)^{0.5} \qquad (1.2)$$

where N_w = 1.33~1.34 (Schiebener *et al.*, 1990; Kirk, 1994a).

(2) At the depth of 10% surface light (Z_{10}):

$$Q_0/Q_d\{R,\theta\} = Q_0/Q_d\{R,0^\circ\} + [\cos 48.6^\circ/(1 - \cos 48.6^\circ)][(1 - \mu_0)/\mu_0]$$
$$*[Q_0/Q_d\{R,89^\circ\} - Q_0/Q_d\{R,0^\circ\}] \qquad (1.3)$$

The equation 1.3 will further break down for different R ranges, where

$$Q_0/Q_d\{R,0^\circ\} = [1 + (28.0 - 50.5R)R]^{0.5} \quad (1.4)$$

$$Q_0/Q_d\{R,89^\circ\} = 1.512[1 + (7.39 - 149R + 1376R^2)R] \quad (1.5)$$

if $0 \leq R \leq 0.055$ and

$$Q_0/Q_d(R,89^\circ) = 1.60 + 3.43R \quad (1.6)$$

if $0.055 \leq R \leq 0.14$.

(3) At the depth of 1% surface light (Z_1):

there are two sets of equations corresponding to different R ranges,

where if $0 \leq R \leq 0.055$,

$$Q_0/Q_d\{R,\theta\} = Q_0/Q_d\{R,0^\circ\}' + [\cos 48.6^\circ/(1 - \cos 48.6^\circ)][(1 - \mu_0)/\mu_0]$$
$$*[Q_0/Q_d(R,89^\circ)' - Q_0/Q_d(R,0^\circ)'] \quad (1.7)$$

where

$$Q_0/Q_d\{R,0^\circ\}' = [1 + (39.1 - 176R)R]^{0.5} \quad (1.8)$$

$$Q_0/Q_d\{R,89^\circ\}' = 1.512[1+ (-2.10 + 117R - 582R^2)R]^{0.8} \quad (1.9)$$

if $0.055 \leq R \leq 0.14$, then

$$Q_0/Q_d\{R,\theta\} = 1.37 + 4.93R. \quad (1.10)$$

Model B.

Model B was developed based on the result of the suggestion by Kirk (1994 a &b) that K_0 is approximately equal to K_d and thus Q_0/Q_d ratio is nearly constant through the water column at a give time of day. Therefore, the following equation was written to estimate the Q_0/Q_d ratio at a given time of day with just one single known ratio of Q_0/Q_d accurately estimated or measured at any one depth i:

$$Q_0/Q_d(t,z) = Q_0/Q_d\ (t,z_i) \quad (2)$$

We want to use two pairs of Q_0/Q_d ratios measured at Z_{100} and Z_{10} to test this model since it is most conveniently to obtain the surface measurement and a measurement at deep layer of water when there is the least effect from air-water interface. Therefore, two sub-models of B1 and B2 are derived:

$$B1: \quad Q_0/Q_d(t,z) = Q_0/Q_d\ (t,z_{100}) \tag{2.1}$$

$$B2: \quad Q_0/Q_d(t,z) = Q_0/Q_d\ (t,z_{10}) \tag{2.2}$$

2.3. Instruments

The LI-COR sensors with LI-COR data logger (model LI-1000 and serial no. LDL1392) and two PUV500 profilers have been employed in field measurement. As shown in figure 8, the sensors set included two LI-COR lowering frames fixed with two cosine sensors (model LI-192SA), of which one faced down (serial no. UWQ4001, multiplier = -272.3 cal. 3/92) detecting upwelling irradiance and the other faced up (serial no. UWQ4013, multiplier = 279.07 cal. 3/92) detecting downwelling irradiance, and one scalar sensor (model Li-193SA, serial no. SPQA1644, multiplier = -255.52 cal. 5/94) detecting the scalar irradiance. The two PUV500 were used one facing up (#9213) to measure Q_d and the other facing down to measure Q_u.

The Q_u measurements were increased by 10% after intercalibration with Q_d and PUV500 showed calibration error of 10% in 10/94. The Q_0 sensor (serial no. UWQ1564, multiplier = -252.33 cal. 10/93) used in fall 1993 and spring and early summer of 1994 was found broken in May 1994. It was replaced at beginning of June 1994.

2.4. Data Collection

Three types of underwater irradiances, Q_d, Q_u, and Q_0, have been measured in

Lake Giles and Lake Lacawac (Table 2: p.). The complete simultaneous measurements of Q_d, Q_u, and Q_0 were obtained since September of 1994 with the LI-COR submersible irradiance meter in both lakes. The data were collected at 1-meter depth intervals (five points stored in the data logger per depth) through the water column. In spring and summer of 1994, the R was continuously measured at 1 meter depth interval in both lakes, some of which are available with simultaneous measurements of Q_0 and Q_d. In 1993, the irradiance reflectance is frequently measured in L. Giles and in L. Lacawac with the profiler PUV500 (normal profiles followed by "inverted profiles). The first simultaneous measurements of Q_0 and Q_d were obtained in L. Giles in November 1993 (with scalar sensor SPQA1564) but no simultaneous R measurements available.

The time of each sample were recorded accurately with the LI-COR meter; the latitudes and longitudes and sun angle (elevation above horizon) of each lake were calculated with the "SCOUT" Global Positioning System (serial no. 0010002B8D), the product of Trimble Navigation Limited. Local time was adjusted to UTC for the GPS unit by adding 4 hours for EDT and 5 hours for EST.

3. RESULTS.

3.1. The Measurements of the Q_0/Q_d Ratio

The Q_0/Q_d ratios are measured in Lake Giles (Fig. 9a) and Lacawac (Fig. 9b) through September of 1994 to February of 1995 (Table 3). It is shown that the average ratios through water column are ranged from 1.40 to 1.54 with an average of 1.47 in Giles, and from 1.34 to 1.61 with an average of 1.48 in Lacawac. The average standard

deviations of 0.31 and 0.14 in Giles and Lacawac, respectively, indicate that the variation of the Q_0/Q_d ratio with depths is smaller in Lacawac than in Giles.

3.2. Testing Model A.

3.2.1. Model A: effect of irradiance reflectance (R)

Low values and small spatial and seasonal changes of R were found in L. Giles and L. Lacawac in 1993 and 1994 (Fig.10). In 1994, for instance, through the water column, the irradiance reflectance varied from 0.015 to 0.049 in L. Giles, 0.004 to 0.016 in L. Lacawac, all smaller than 0.055. Table 4 shows the averages and ranges of R at the depths of Z_{100}, Z_{10}, and Z_1, respectively, in each lake. In the clear lake, L. Giles, the values of the irradiance reflectance are higher than in L. Lacawac.

The R measurements in Lake Giles through the year of 1993 about 35% lower, as a whole, than that in 1994. The PUV500 was used *in situ* in 1993, whereas the LI-COR meter was used in 1994. Some other measurements from the PUV always tends to be lower than that from the LI-COR so that we need further to confirm that different instruments used caused the shift of the irradiance reflectance in the different years.

The average, minimum, and maximum values of R have been input into the model to test the effect of R on the Q_0/Q_d prediction (Fig.11) under different sun-angles. The highest and lowest sun available at the location of the lakes is $\theta = 18^0$ and 90^0, respectively. At the surface (Z_{100}), the error of Q_0/Q_d prediction caused by R variation is smaller (Table.5) than in the lower layers of the water (e.g. Z_{10} and Z_1) under different sun-angles. At same depth, the error of the prediction with the average R's increases when the sun is higher.

3.2.2. Model A: effect of sun-angle (θ).

If an average sun-angle $\theta = 45^0$ is assumed on each sampling date, the error of Q_0/Q_d prediction is up to 29% at surface (Z_{100}), and 2~24% at water layer lower than Z_{10} (Table 6). The effect of sun-angle is also shown in Figure 12.

3.2.3. Model A: predictions and errors.

In the prediction with model A, the variation of R in the lakes is ignored, instead, the annual averages of R's at Z_{100}, Z_{10}, and Z_1 are used since that the error in the Q_0/Q_d prediction caused by R is considered small (less than 2% at the surface of the waters where light intensity is the highest, and less than 13% through the rest of the water columns if the average values are used replacing the actual R). In contrast, the effect of sun-angle has to be taken into account.

The Q_0/Q_d ratios at the depths of Z_{100}, Z_{10}, and Z_1 in each lake and sampling date are computed in model A. The ratios at depths between the three particular depths are interpreted linearly in Giles (Fig.13) and Lacawac (Fig. 14); no predictions at depth beyond are available. The averages of the ratio with depths vary from 1.34 to 1.53 in deferent sampling dates with an overall average of 1.44 in Giles, and from 1.37 to 1.53 with an overall average of 1.47 in Lacawac (Table 7). Errors of the prediction at each depth and each sampling time (each profile), $E_{z,t}$, are estimated by the percentage of the difference of the predicted and the measured ratio to the measured ratio, i.e.,

$$E_{z,t} = 100\% * [Q_0/Q_d(\text{predicted}) - Q_0/Q_d(\text{measured})] / Q_0/Q_d(\text{measured}).$$

Table 8 shows that the overall error (average of absolute values, measured-predicted) over depths and time is 12.87% at surface and 6.24% at lower depths in Giles;

15.12% at surface and 10.16% at lower depths in Lacawac. It also shows that the overall errors are (about 35-100%) greater at the surface than at the lower layers of waters in all the lakes; and the prediction seems better in Giles (the more clear lake) than in Lacawac.

Some "repair" of the raw data was required to eliminate either the cloud-effect (in the two replicates in 9/20/94 and the single profile in 11/22/94) or an operational error (placed sensors at the opening of drilled ice hole instead under the ice in 2/21/95) all in Giles. Fig.13d shows the improved prediction in Lake Giles on 11/22/94 which eliminated cloud-effect by fixing the Q_d and Q_0 records. Average K_d or K_0 was used to extrapolate Q_d or Q_0 to the surface.

3.3. Testing Model B1 & B2.

In both model B1 and B2, the actual ratio measured at surface (Z_{100+}) and the depth of 10% Q_d are simply used as the prediction for all depths in Giles (Fig.13) and Lacawac (Fig. 14) assuming that the ratio is constant through each water column. The predicted Q_0/Q_d ratios are listed in Table 9.

The absolute errors in model B1 in table 10 show that the average error over the depths below the surface is mostly higher than 10%; and one-third show errors higher than 25%. The overall averages and ranges show that there is little difference between the two lakes.

When the ratio is determined below the surface (model B2), the error shown in table 10 is always lower than 11% below the surface. This is much lower than the error at surface (mostly > 10% and 1/3 of which > 20%. The overall averages and ranges show that there is little difference between the two lakes (Table.11).

4. DISCUSSION

Two examples of estimation of the scalar irradiance from the predicted ratios is shown in Figure 15. The performances of model A and B2 are similar (Table 12): the overall average errors below surface are always within 8%, but 14.5% at surface; and the fact of that large error existing in B1 but not B2 probably indicates that the large error is most likely caused by the inaccuracy of surface measurements but not by the method; additionally, model B seems perform better than model A given that one single ratio can be measured or estimated accurately.

To more accurately evaluate the performances of the models, a t-test of the "comparison of paired samples" (Snedecor & Cochran, 1989) has been run to test whether the differences between the ratios predicted by each model and that measured at each depth are significant (Table 13).

It is shown that, in general, model A and model B2 performed similarly and both better than model B1. The inconsistency of the evaluations by absolute error and by t-test is caused by the trend of uneven distributions of actual errors about the observed means of differences in model B predictions which can not be detected by the absolute error method. The fact that 50% of the predictions are significantly different from the measurements indicates both the imperfect of the models and unreliability of at least the surface measurements of the ratio. All five accepted cases with B2 occurred in Lacawac and three out of five with A occurred in Giles. This may imply that model A performed about same in both lakes, while model B2 performed worse in a more clear lake, such as Giles.

An ideal model might share the strengths in both model A and B, i.e., with smaller errors yet still independent from the scalar light sensor. Howard R. Gordon (1989) shows that the surface Q_0/Q_d ratio (D_0) can be estimated by measuring only the ratio of direct sunlight to the overall sunlight. Further research is definitely necessary for exploring, the combination of D_0 and model B. This approach would require the fewest measurements and calculation might result in the best prediction while still independent from using a scalar sensor. It requires only the recording of skylight with direct sunlight shaded.

5. CONCLUSIONS

The overall averages of measured ratio were 1.47 in Giles and 1.48 in Lacawac; the ratio varied from 1.08 to 2.25 in Giles and 1.10 to 1.88 in Lacawac. Sun-angle had the greatest impact on the ratio, followed by sky and wind conditions, finally irradiance reflectance.

The predictions of model A deviate from the measurements by ±5-14% over the dates tested; and those of model B deviates by ±3-11%. A single depth could differ by a much greater error. The significant errors of the predictions are partly caused by the rapid fluctuations in the light fields not fully recorded by the instrument, especially at upper layers of the waters. It appears to be true that the accuracy of model tend to be better than the actual measurements.

TABLES

Table 1. General availabilities of the scalar and cosine sensors.

Characteristics	Q_0 Sensor	Q_d Sensor
Fragile	Yes	No
Shading Problem	Great	Small
Available with a Light Profiler	No	Yes

Table 2. Data Availability.

MEASUREMENTS		R (Q_u & Q_d)		Q_0 & Q_d	
LAKE		Giles	Lacawac	Giles	Lacawac
METHOD	PUV500	04/20/93 05/12/93 08/27/93 09/13/93	 08/03/93	 11/16/93	
	LI-COR	04/26/94 05/09/94 05/26/94 07/07/94	 05/09/94 05/26/94 05/27/94 06/06/94		 05/26/94 05/27/94 06/03/94 06/06/94
	LI-COR SIMUL-TANEOUS	08/25/94 09/20/94 10/18/94 11/22/94 02/21/95	 09/20/94 10/18/94 11/22/94 02/21/95	08/25/94 09/20/94 10/18/94 11/22/94 02/21/95	 09/20/94 10/18/94 10/24/94 11/22/94 02/21/95

Table 3. The measurements of the Q_0/Q_d ratio: averages and ranges.

DATE	LAKE	Q_0/Q_d (Avg. all depths)	RANGE (# of Depths)
9/20/94	GILES REP.1	1.52	1.08, 1.83 (22)
	GILES REP.2	1.45	1.18, 2.25 (19)
	LACAWAC	1.62	1.32, 1.88 (9)
10/18/94	GILES	1.40	1.35, 1.51 (22)
	LACAWAC	1.34	1.25, 1.40 (10)
10/24/94	LACAWAC	1.50	1.10, 1.65 (11)
11/22/94	GILES	1.54	1.32, 2.22 (19)
	LACAWAC	1.47	1.28, 1.82 (10)
2/21/95	GILES	1.44	1.38, 2.00 (22)
	LACAWAC	1.48	1.32, 1.70 (9)
ALL DATES	GILES	1.47	1.08, 2.25
	LACAWAC	1.48	1.10, 1.88

Table.4 The irradiance reflectance (R) in the Pocono Lakes.

Lake	Giles	Lacawac
Depth	AVG (Range)	AVG (Range)
Z_{100}	0.017 (0.014,0.017)	0.006 (0.004,0.006)
Z_{10}	0.030 (0.018, 0.027)	0.008 (0.005, 0.009)
Z_1	0.034 (0.023, 0.033)	0.010 (0.004, 0.009)

Table.5 Error of Q_0/Q_d prediction caused by using average R (%).

Lake Name	Giles	Lacawac
Z_{100}	-0.7 ~ +1	-1.2 ~ +1.4
Z_{10}	-3 ~ +13	-1.9 ~ +5.8
Z_1	-2.4 ~ +7.8	-1.9 ~ +5.8

Table 6. Error of Q_0/Q_d prediction when sun-angle 45° used instead of actual sun-angle.

Lake Name	Giles	Lacawac
Z_{100}	-14.4 ~ +29.1	-14.4 ~ +29.1
Z_{10}	-7.2 ~ +15.6	-11.2 ~ +24.1
Z_1	-2.1 ~ +4.6	-7.8 ~ +16.8

Table 7. The predictions of the ratio by model A: averages and ranges.

DATE	LAKE	Q_0/Q_d (Avg. all depths)	RANGE (# of Depth)
9/20/94	GILES REP.1	1.39	1.26, 1.49 (19)
	GILES REP.2	1.34	1.18, 1.47 (19)
	LACAWAC	1.44	1.42, 1.46 (7)
10/18/94	GILES	1.45	1.32, 1.50 (20)
	LACAWAC	1.48	1.44, 1.50 (7)
10/24/94	LACAWAC	1.37	1.35, 1.39 (6)
11/22/94	GILES	1.53	1.46, 1.58 (19)
	LACAWAC	1.54	1.48, 1.56 (5)
2/21/95	GILES	1.47	1.31, 1.50 (13)
	LACAWAC	1.37	1.35, 1.39 (6)
ALL DATES	GILES	1.44	1.18, 1.58
	LACAWAC	1.47	1.35, 1.56

Table 8. The Error of Model A (predicted - measured as % of measured).

Date	Lake	Surface	Below Surface
9/20/94	Giles-Rep.1	-12.52	10.70
	Giles-Rep.2	-2.23	4.06
	Lacawac	-6.20	13.60
10/18/94	Giles	-11.80	6.19
	Lacawac	-18.01	10.02
10/24/94	Lacawac	+22.61	10.77
11/22/94	Giles	-26.29	5.40
	Lacawac	-14.68	6.24
2/21/95	Giles	-11.55	4.85
	Lacawac	-14.11	10.17
Overall Average Error (Range)	Giles	12.9 (-26, +2)	6.2 (-12, +16)
	Lacawac	15.1 (-18, +23)	10.2 (-23, +14)

Table 9. The predictions of the ratio by model B1 and B2: Averaged with depths.

DATE	LAKE	Q_0/Q_d (model B1)	Q_0/Q_d (model B2)
9/20/94	GILES REP.1	1.60	1.43
	GILES REP.2	1.40	1.15
	LACAWAC	1.53	1.71
10/18/94	GILES	1.35	1.50
	LACAWAC	1.25	1.38
10/24/94	LACAWAC	1.10	1.54
11/22/94	GILES	1.60	1.97
	LACAWAC	1.82	1.37
2/21/95	GILES	1.47	1.49
	LACAWAC	1.57	1.58
ALL DATES	GILES	1.51	1.49
	LACAWAC	1.45	1.51

Table 10. Average Errors (%) in B1 (computed as in Table 8).

Date	Lake	Surface	Below Surface
9/20/94	Giles-Rep.1	Defined 0	12.42
	Giles-Rep.2	Defined 0	13.93
	Lacawac	Defined 0	12.58
10/18/94	Giles	Defined 0	7.54
	Lacawac	Defined 0	6.61
10/24/94	Lacawac	Defined 0	28.52
11/22/94	Giles	Defined 0	35.36
	Lacawac	Defined 0	25.93
2/21/95	Giles	Defined 0	3.51
	Lacawac	Defined 0	6.08
Overall Average Error (Range)	Giles	Defined 0	14.55 (-18,+50)
	Lacawac	Defined 0	15.94 (-18,+40)

Table 11. Average Errors (%) in B2 (computed as in Table 8).

Date	Lake	Surface	Below Surface
9/20/94	Giles-Rep.1	+11.79	10.84
	Giles-Rep.2	+21.47	7.71
	Lacawac	+11.11	10.28
10/18/94	Giles	-9.74	2.95
	Lacawac	+9.95	3.88
10/24/94	Lacawac	+39.69	5.15
11/22/94	Giles	-18.92	9.75
	Lacawac	-24.86	5.96
2/21/95	Giles	-1.08	2.55
	Lacawac	+0.43	6.19
Overall Average Error (Range)	Giles	12.24 (-19, +21)	6.76 (-12, +27)
	Lacawac	17.21 (-25, +40)	6.29 (-12, +28)

Table 12. Comparison of model errors.

Depth	Item	Model A	Model B1	Model B2
Surface	Overall Average	± 14%	Defined 0%	± 14.5%
	Range w. Depths	-26, +23	-- --	-25, +40
Below surface	Overall Average	± 8%	± 15.5%	± 6.5%
	Range w. Depths	-23, +16	-28, +50	-12,+28

Table 13. Statistic test of the models.

DATE	LAKE	PROBABILITY of H_0: Model = Measurement		
		*=Sig.Diff. @p<=0.05; **=Sig.Diff.@p<=0.005		
		Model A	Model B1	Model B2
9/20/94	GILES REP.1	*		*
	GILES REP. 2		**	*
	LACAWAC	*		
10/18/94	GILES	**	**	**
	LACAWAC	**	*	
10/24/94	LACAWAC		**	
11/22/94	GILES		**	**
	LACAWAC		*	
2/21/95	GILES		**	*
	LACAWAC	*		

Table 14. Application and limitation of model A & B.

MODEL	A	B
AVG ERROR, %	5-14	3-11
GOOD FEATURE	1) No Q_0 sensor required; 2) Change of ratio with depths available.	1) Simple to compute; 2) For any weather condition; 3) All depths available.
BAD FEATURE	1) Measurements of Q_a required for each depth & lake; 2) Complicated computation; 3) Small H_2O clarity required for best performance; 4) Non-available at depth below Z_1.	1) Q_0 sensor required; 2) Accurate measurements of Q_0 & Q_d required; 3) Assume constant ratio with depths; 4) Performs better in less clear waters.

FIGURES

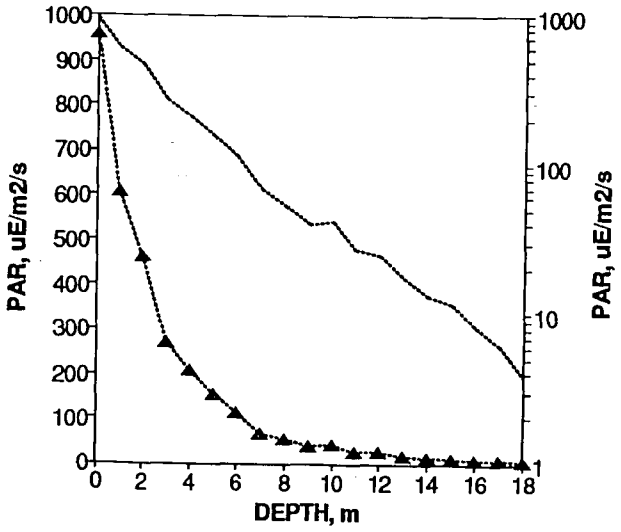

Figure 1: *Underwater light availability.*

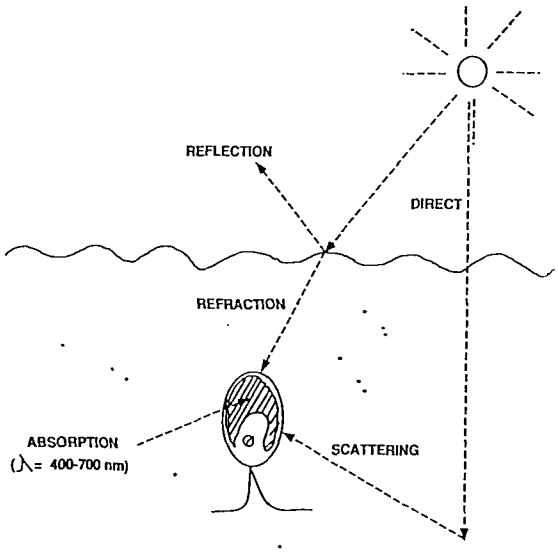

Figure 2: *Optical processes in atmosphere-lake system.*

(a)

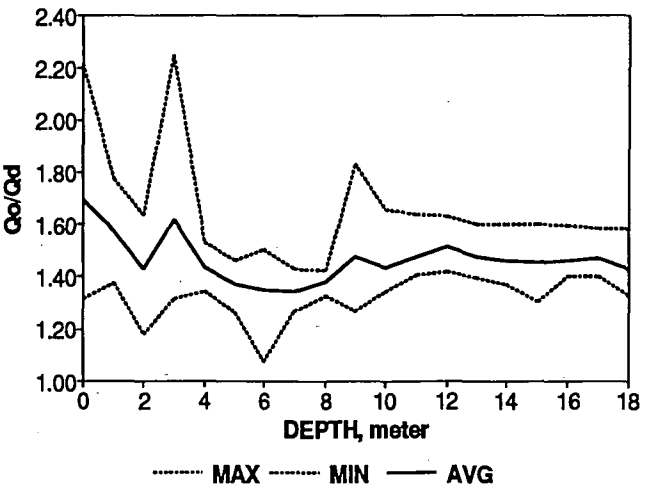

(b)

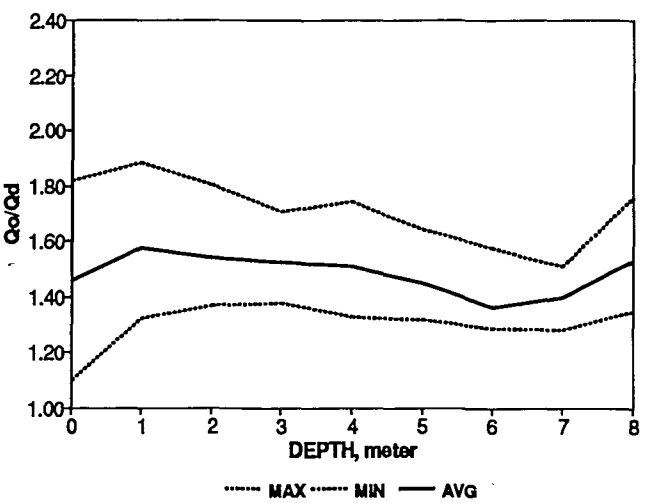

Figure 3: *Variation of the Q_o/Q_d ratio in Giles (a) and Lacawac (b).*

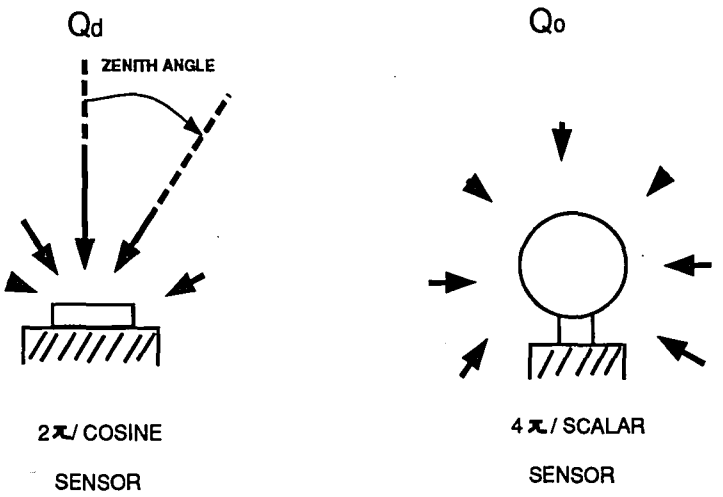

Figure 4: COMPARISON OF LIGHT SENSORS

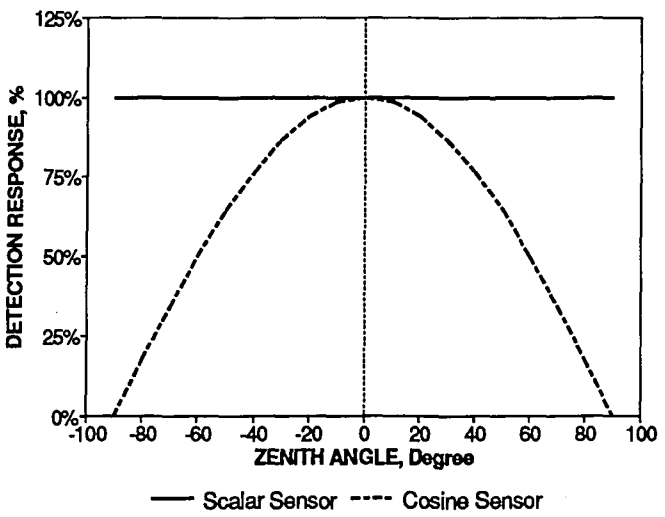

Figure 5: *Responses of the cosine and scalar sensors.*

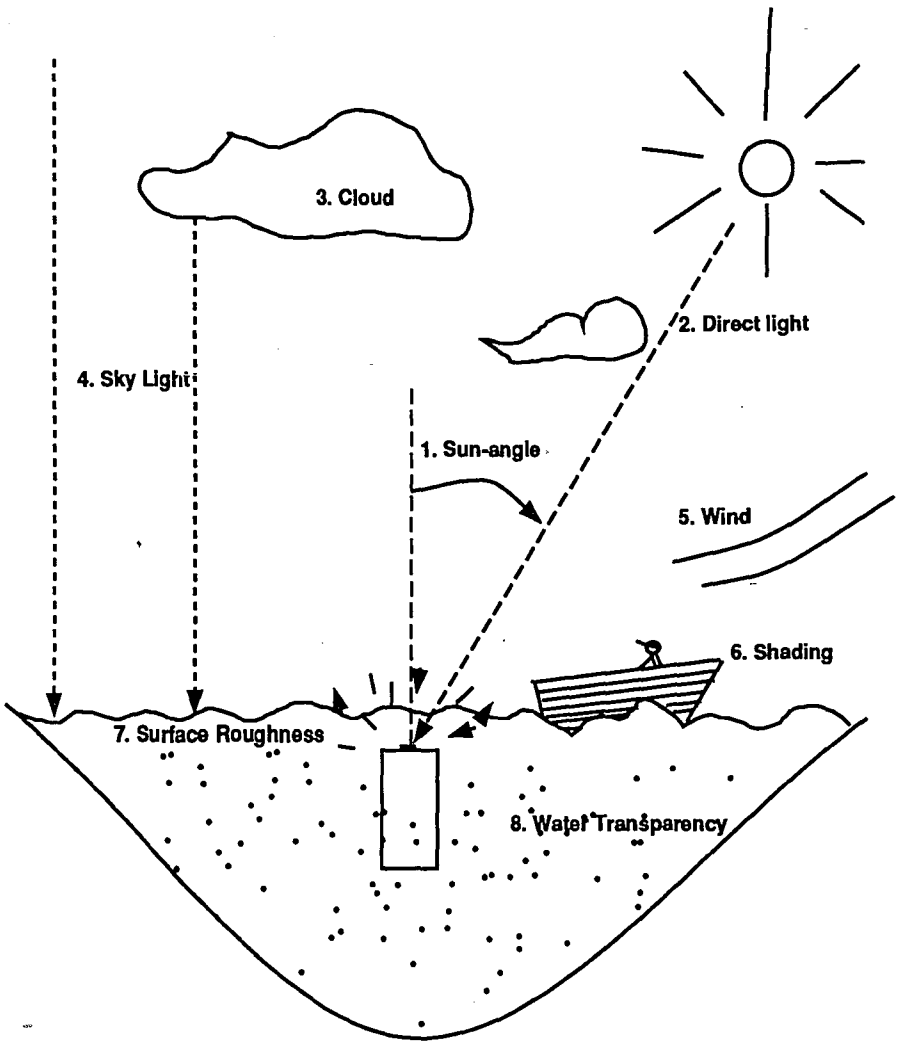

Figure 6: ENVIRONMENTAL EFFECTS ON Qo/Qd RATIO

(a)

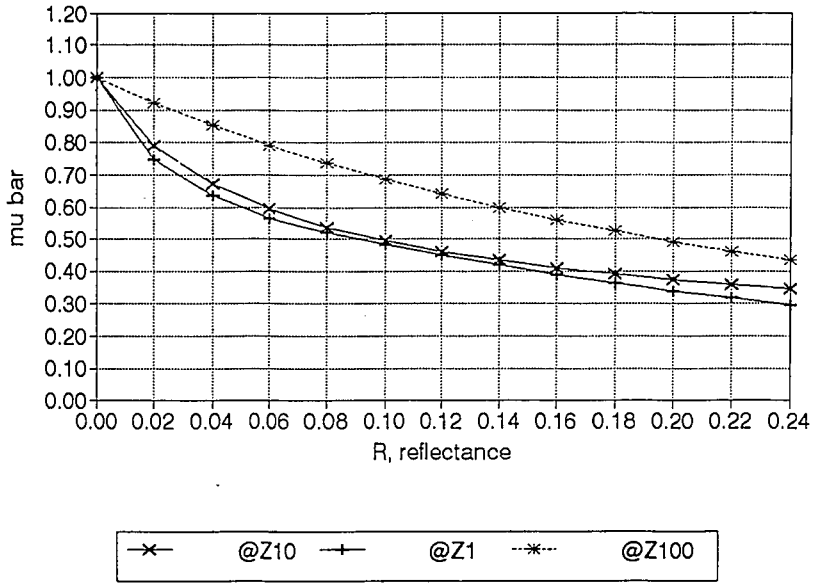

(b)

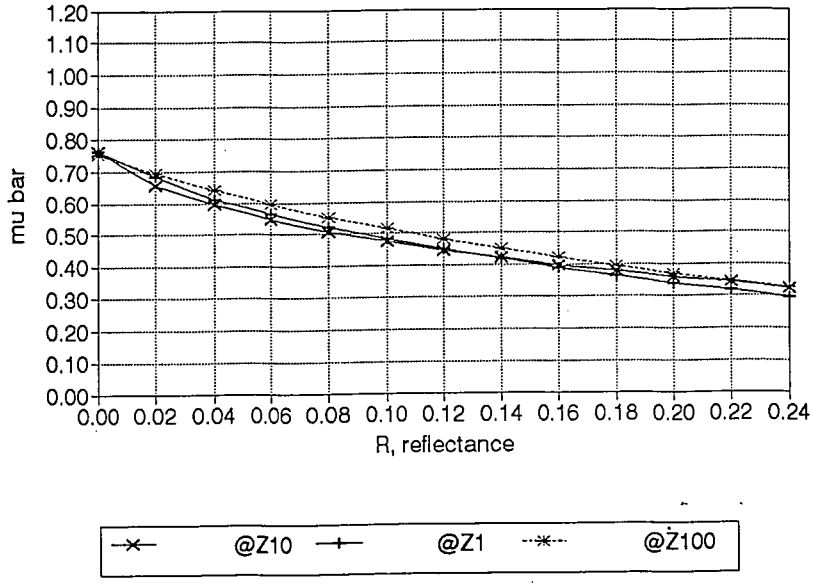

Figure 7: *Model A: a Monte Carlo computer simulation of underwater light field.*

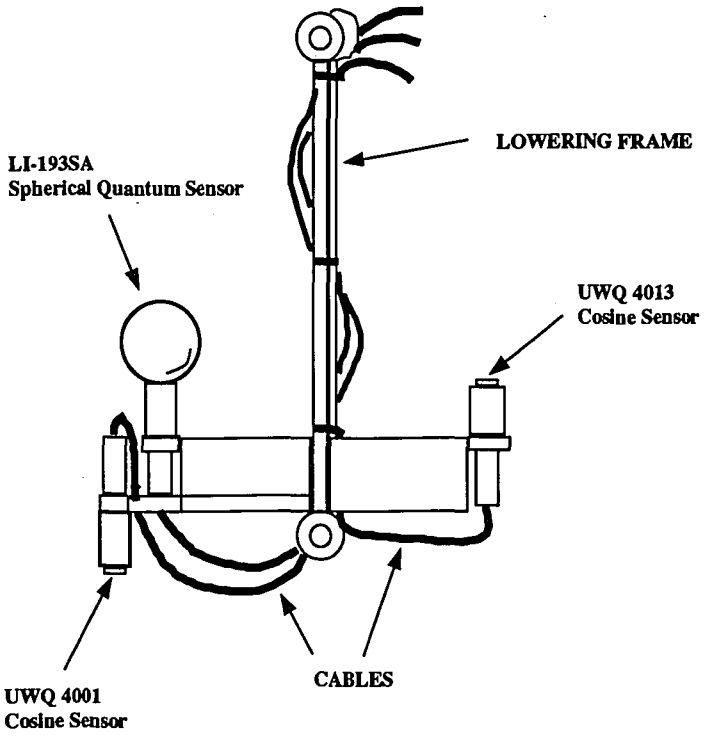

Figure 8: LI-COR SUBMERSIBLE IRRADIANCE METER

(a)

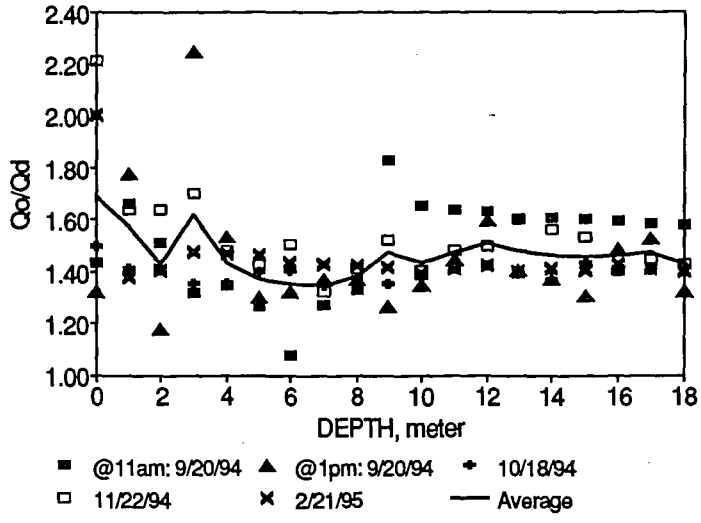

(b)

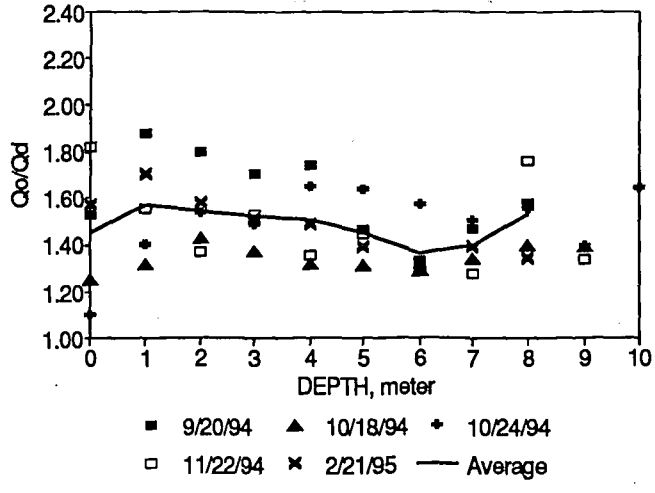

Figure 9: *The measurements of the Q_o/Q_d ratio in Giles (a) and Lacawac (b).*

(a)

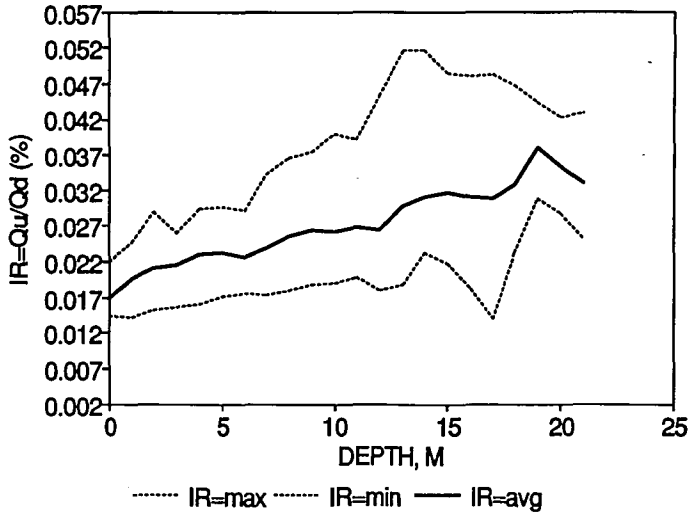

(b)

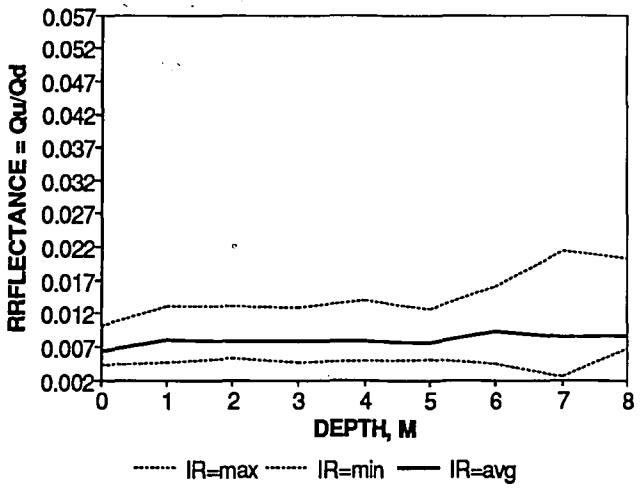

Figure 10: *Irradiance reflectances in Giles (a) and Lacawac (b).*

(a)

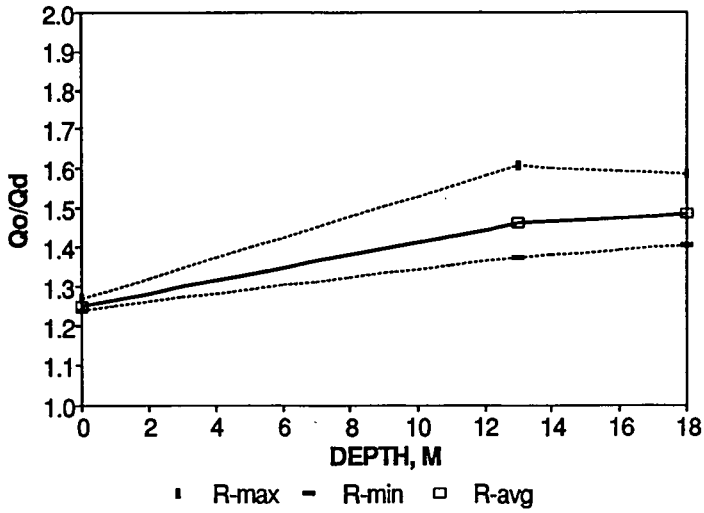

(b)

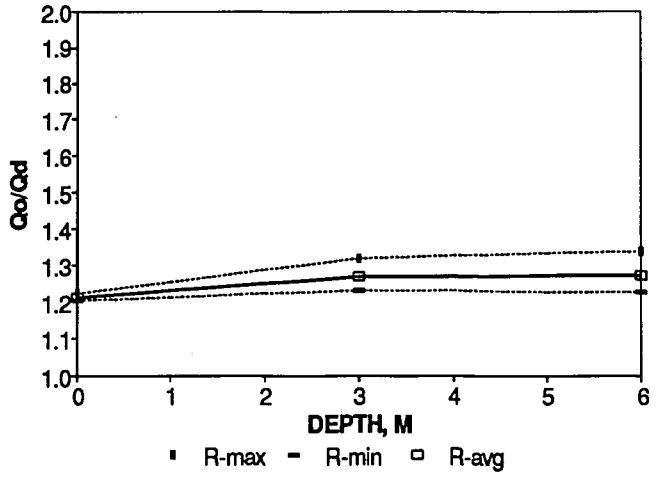

Figure 11: *The effect of reflectance on the ratio in Giles (a) and Lacawac (b).*

(a)

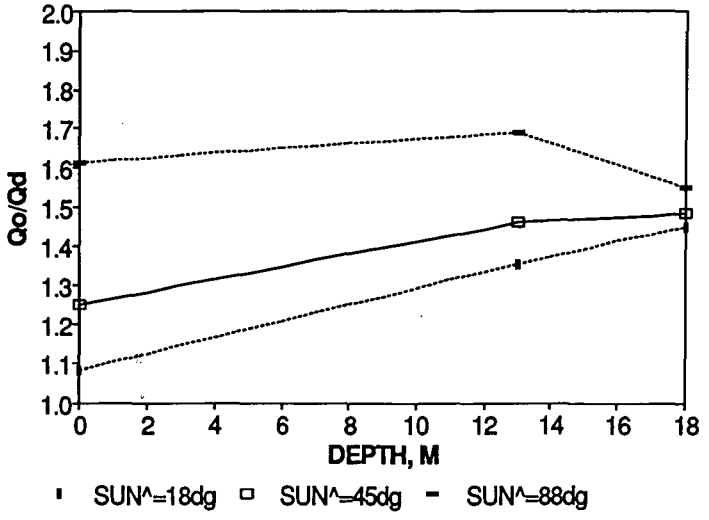

(b)

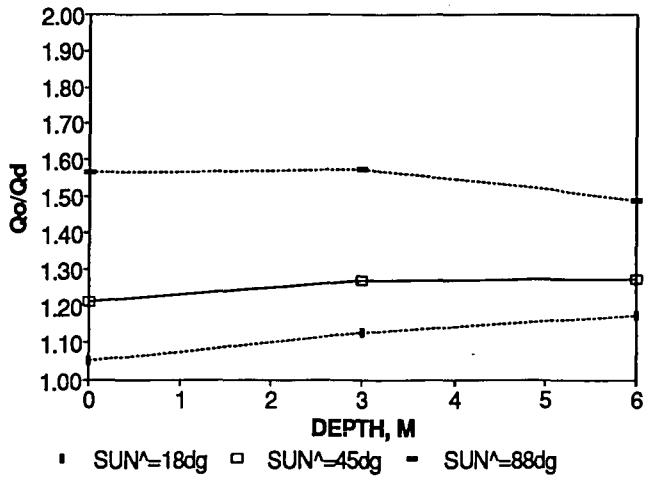

Figure 12: *The effect of sun-angle on the ratio in Giles (a) and Lacawac (b).*

(Figure 13 a)

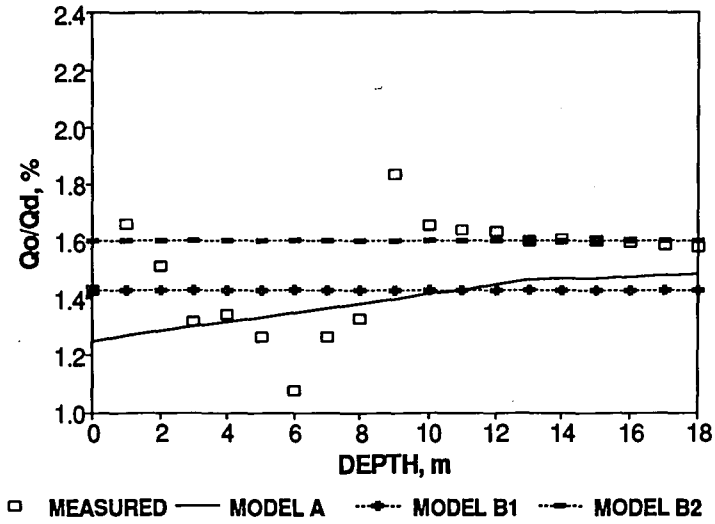

(Figure 13 b)

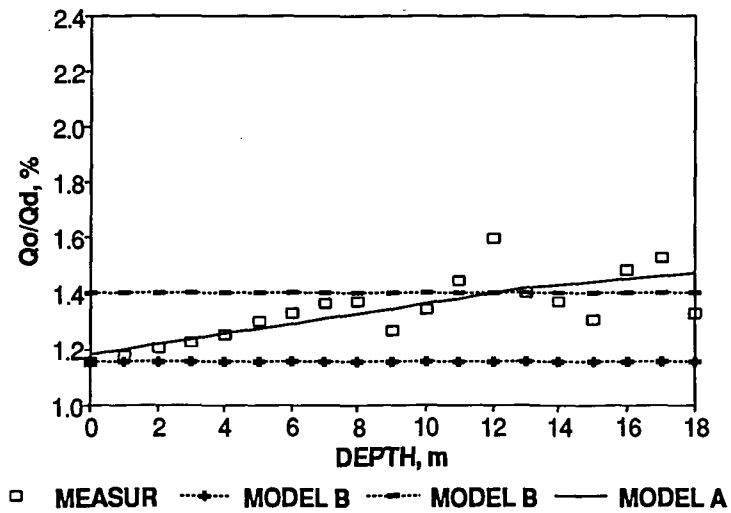

(Figure 13c)

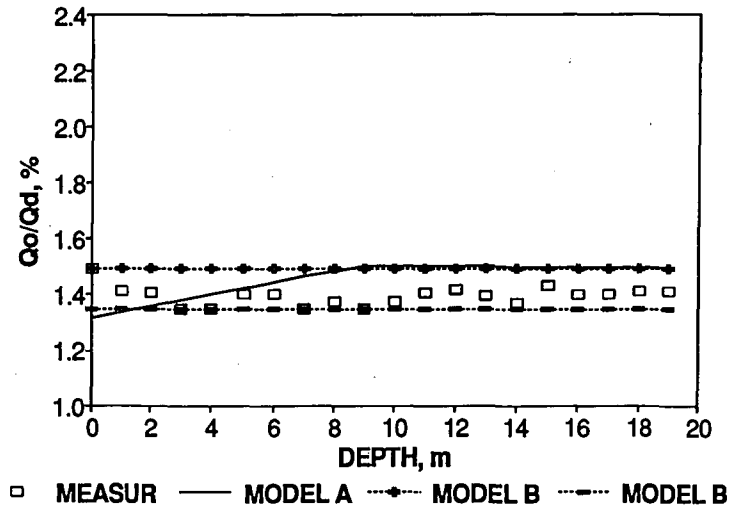

(Figure 13 d)

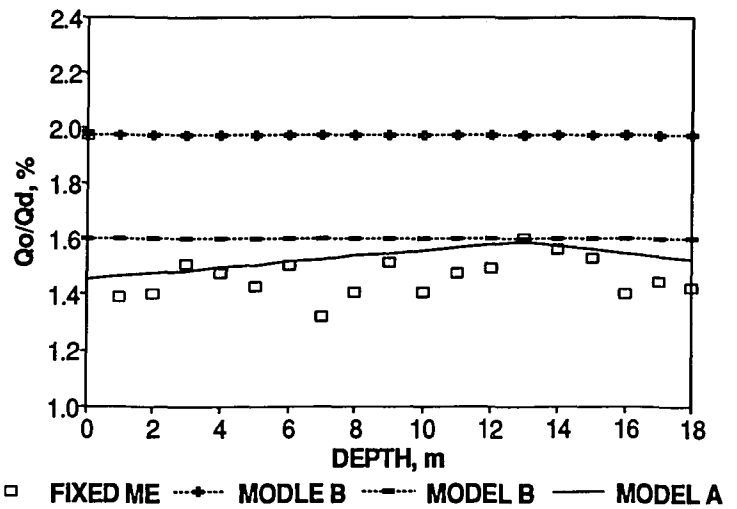

(Figure 13 e)

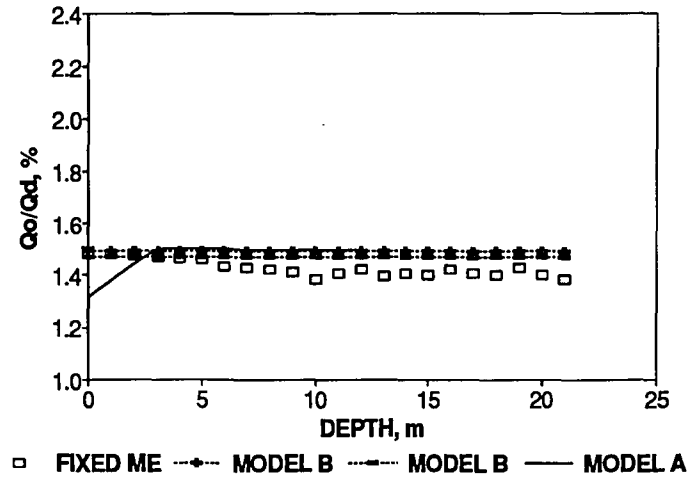

Figure 13: *The predictions of the ratio with model A1, B1, and B2 in Giles (a-e).*

(Figure 14 a)

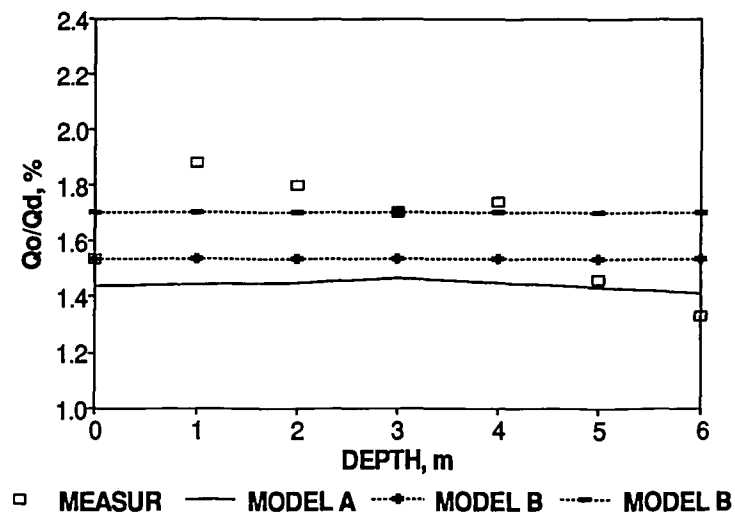

(Figure 14 b)

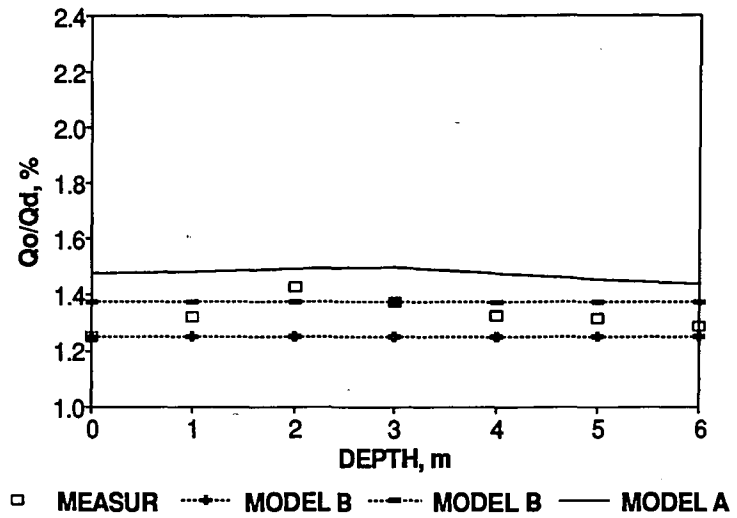

(Figure 14 c)

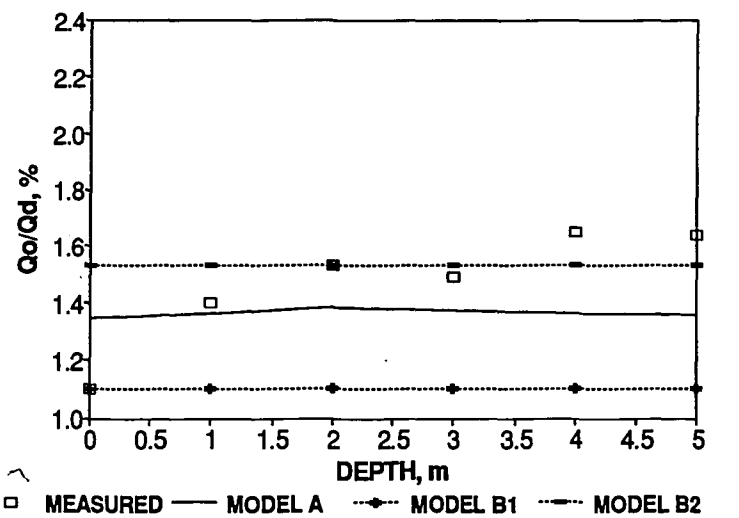

(Figure 14 d)

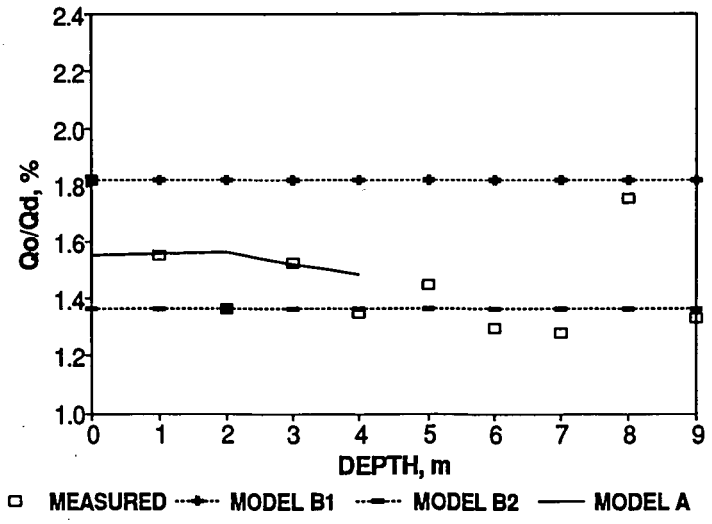

(Figure 14 e)

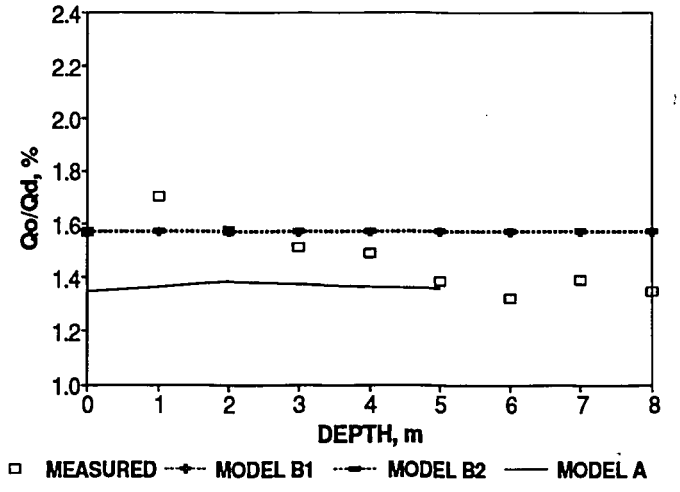

Figure 14: *The predictions of the ratio with model A, B1, and B2 in Lacawac (a-e).*

(Figure 15 a)

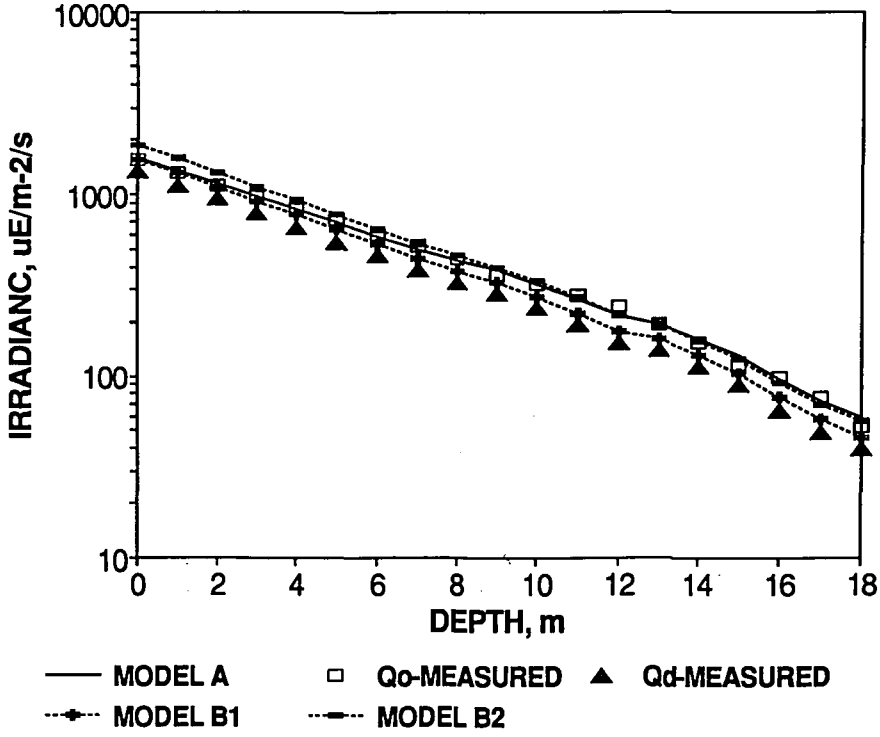
10000
1000
100
10
IRRADIANC, uE/m-2/s
0
2
4
6
8
10
12
14
16
18
DEPTH, m
MODEL A
Qo-MEASURED
Qd-MEASURED
MODEL B1
MODEL B2

(Figure 15 b)

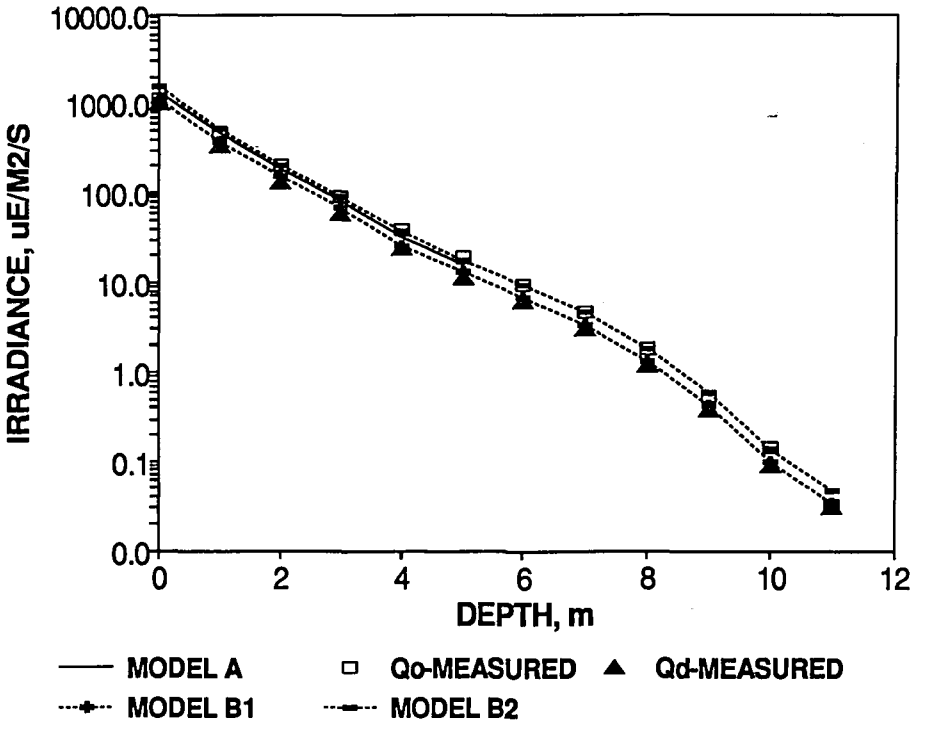

Figure 15: *Estimation of the Q_0 irradiance in Giles (a) and Lacawac (b).*

REFERENCES

ANON, 1986. LI-COR Underwater radiation sensors, Type SA instruction manual. Publication No. 8609-57. LI-COR inc..

ANON, 1993. A global navigation system in the palm of your hand, SCOUT GPS™, user's guide. Trimble Navigation Limited.

Booth C. R., 1975. The design and evaluation of a measurement system for photosynthetically active quantum scalar irradiance.

Gordon H., 1987. A bio-optical model describing the distribution of irradiance at the sea surface resulting from a point source embedded in the ocean. Appl. Opt. 26, 4133-4148.

--, 1989. Can the Lambert-Beer law be applied to the diffuse attenuatio coefficient of ocean water? Limnol. Oceanogr., 34(8), 1389-1409.

Jerome J. H. *et al.*, 1988. Utilizing the components of vector irradiance to estimate the scalar irradiance in natural waters. Appl. Opt. 27(19), 4012-4018.

Jordan M. B., 1988. A new submersible recording scalar light sensor array. Deep-Sea Res. 35(8), 1411-1423.

Kirk J. T. O., 1981a. Monte Carlo procedure for simulating the penetration of light into natural waters. Div. Plant Industry Tech. Paper 36 (Commonwealth Scientific and Industrial Research Organization, Canberra, Australia).

--, 1981b. Monte Carlo study of the nature of the underwater light field in, and the relationships between optical properties of, turbid yellow waters. Aust. J. Mar. Freshwater Res. 32, 517-532.

--, 1994a. Light & photosynthesis in aquatic ecosystems (2nd edition). Cambridge University Press. 6-12; 38-45;151-154.

--, 1994b. Estimation of the absorption and the scattering coefficients of natural waters by use of underwater irradiance measurements. Appl. Opt. 33, 3276-.

Mobley C., 1989. A numerical model for the computation of radiance distributions in natural waters with wind-roughened surfaces, Limnol. Oceanogr. 34, 1473-1483.

Mobley C. *et al.*, 1993. Comparison of numerical models for computing underwater light field. Appl. Opt. 32, 7484-.

Moeller R. E., Williamson C. E., Hargreaves B. R., & Morris D. P., 1995. Limnology of lakes Lacawac, Giles, and Waynewood 1989-93: an introduction to the core lakes of the Pocono Comparative Lakes Program. Lehigh University. 44 pp.

Morel A., 1991. Light and marine photosynthesis: a spectral model with geochemical and climatological implications. Limnol. Oceanogr. 26, 263-306.

Morrow J., 1993. Terminology and units: natural fluorescence calculations using the PNF-300 and PUV-500. (Unpublished notes).

Plass G. & Kattawar G., 1969. Radiative transfer in an atmosphere-ocean system. Appl. Opt. 8, 455-466.

-- & --, 1972. Monte Carlo calculations of radiative transfer in the earth's atmosphere ocean system:I. Flux in the atmosphere and ocean. J. Phys. Oceanogr. 2, 139-145.

Platt T. & Sathyendranath S., 1988. Oceanic Primary production: estimatio by remote sensing at local and regional scales, Science 241, 1613-1620.

Preisendorfer R., 1988. Eigenmatrix representations of radiance distributions in layered natural waters with wind-roughened surfaces. NOAA Tech. Meno. ERL PMEL-76 (NTIS PB88-188701) (Pacific Marine Environmental Laboratory, Seattle, Wash.).

Prieur L. & Sathyendranath S., 1981. An optical Classification of Coastal and oceanic waters based on the specific spectral absorption curves of phytoplankton pigments, dissolved organic matter and other particulate materials. Limnol. Oceanogr. 26, 671.

Schieberner P. *et al.*, 1990. Refractive index of water and steam as function of wavelength, temperature, and density. J. Phys. Chem. Ref. Data. 19(3), 679-715.

Smith R. C. *et al.*, 1989. Bio-optical modeling of photosynthetic production in coastal waters. Limnol. Oceanogr., 34 (8), 1524-1544.

Snedecor G. W. & Cochran W. G., 1989. Statistical Methods (8th edition). Iowa State University Press. 503, 83-88.

Stavn R. & Weidemann A., 1988. Optical modeling of clear ocean light fields: Raman Scattering effects. Appl. Opt. 27, 4002-4011.

SIGNIFICANT SYMBOLS

a Total absorption coefficient, m^{-1}

b Total scattering coefficient, m^{-1}

c Total attenuatio coefficient, m^{-1}

K_d Diffusion attenuation coefficient for Q_d, m^{-1}

K_0 Diffusion attenuation coefficient for Q_0, m^{-1}

N_w The refractive index of water

Q Quantum irradiance (light intensity), $\mu E/m^2/s$

Q_d Quantum downwelling irradiance, $\mu E/m^2/s$

Q_0 Quantum scalar irradiance, $\mu E/m^2/s$

Q_u Quantum upwelling irradiance, $\mu E/m^2/s$

R Irradiance reflectance (Q_u/Q_d)

μ-bar Average cosine for the total light ($(Q_d-Q_u)/Q_0$)

θ Solar zenith angle above water surface (= 0 when sun is at zenith)

$Z_{\%}$ Optical depth--the depth represented by percentage of Q at surface (e.g. Z_{10} = depth when Q is 10% of surface irradiance)

Vita

Yin Zhong

Education

M.S. Environmental Science, Lehigh University, Bethlehem, PA, May 1995.

M.S. Physical Geography, Beijing Normal University, Beijing, China, June 1988.

B.S. Geography, Beijing Normal University, Beijing, China, July 1985.

Graduate, The high school of Tsinghua University, Beijing, China, July 1981.

Work Experience

Graduate/Research/Teaching Assistant, Lehigh University, Bethlehem, 1992-1995.

Junior Official, State Land Administration, P.R.C. Dept. of State, November 1988-April 1991.

Associate Lecturer, Beijing Normal University, Beijing, P. R. China, June-November 1988.

Research Assistant, Beijing Normal University, Beijing, P. R. China, September 1985-June 1988.

Publications

Y. Zhong & J. Wu, *Chinese J. Arid Land Res.* 3, 2 (**1990**).

J. Wu, H. Jiang, Q. Tian, & Y. Zhong, *J. Beijing Normal Univ.* Sup.1, 10 (**1988**).

END OF TITLE